0022-3565/09/3311-234–243$20.00
THE JOURNAL OF PHARMACOLOGY AND EXPERIMENTAL THERAPEUTICS
JPET 331:234–243, 2009

Vol. 331, No. 1
153510/3515111
Printed in U.S.A.

Coordinated Regulation of Dimethylarginine Dimethylaminohydrolase-1 and Cationic Amino Acid Transporter-1 by Farnesoid X Receptor in Mouse Liver and Kidney and Its Implication in the Control of Blood Levels of Asymmetric Dimethylarginine

Jiang Li, Annette Wilson, Xiang Gao, Ramalinga Kuruba, Youhua Liu, Samuel Poloyac, Bruce Pitt, Wen Xie, and Song Li

Center for Pharmacogenetics, Department of Pharmaceutical Sciences, School of Pharmacy, University of Pittsburgh, Pittsburgh, Pennsylvania (J.L., A.W., X.G., R.K., S.P., W.X., S.L.); Department of Pathology, School of Medicine, University of Pittsburgh, Pittsburgh, Pennsylvania (Y.L.); and Department of Environmental and Occupational Health, Graduate School of Public Health, University of Pittsburgh, Pittsburgh, Pennsylvania (B.P.)

Received March 16, 2009; accepted July 14, 2009

ABSTRACT

Asymmetric dimethylarginine (ADMA) is a potent endogenous inhibitor of endothelial nitric-oxide synthase (eNOS), and increased plasma concentrations of ADMA have been regarded as a risk factor for a number of cardiovascular diseases. Circulating ADMA is largely taken up by liver and kidney via system y^+ carriers of the cationic amino acid (CAT) family and subsequently metabolized by dimethylarginine dimethylaminohydrolases (DDAHs). As such, agents targeted at enhancing ADMA metabolism may prove to be useful in the prevention and/or treatment of various types of cardiovascular disease. Farnesoid X receptor (FXR) is a member of the nuclear receptor superfamily and plays an important role in the maintenance of cholesterol and bile acid homeostasis. We report here that treatment of mice with an FXR agonist 3-(2,6-dichlorophenyl)-4-(3'-carboxy-2-chlorostilben-4-yl)oxymethyl-5-isopropylisoxazole; GW4064) led to increased expression of DDAH-1 and CAT-1 in both liver and kidney. In cultured human hepatocytes and kidney proximal tubular epithelial cells, GW4064 increased CAT-1 expression, and this was associated with a significant increase in the cellular uptake of ADMA. Promoter analyses suggest that CAT-1 is a likely target of FXR, and a functional FXR response element was found in the promoter region of CAT-1 gene. These data suggest that FXR may play an important role in regulating blood levels of ADMA via coordinated regulation of DDAH-1 and CAT-1 in liver and kidney.

NO is a critical effector molecule in the cardiovascular system and eNOS-derived NO plays an important role in vascular homeostasis (Stuehr, 1997; Dudzinski et al., 2006). Impaired eNOS function is implicated in diabetes mellitus, hypertension, pulmonary hypertension, and other cardiovascular diseases (Schulz et al., 2008).

eNOS activity is regulated in a complex fashion at transcriptional, post-transcriptional, and post-translational levels (Shaul, 2002; Searles, 2006). Asymmetric dimethylarginine (ADMA), a potent endogenous eNOS inhibitor, has also been shown to be critically involved in the control of eNOS-mediated NO production (Böger, 2003; Vallance and Leiper, 2004).

Dimethylarginines originate from the degradation of methylated proteins. Methylation of arginine residues is catalyzed by protein arginine methyltransferases, giving rise to three forms of methylarginines: *N*-monomethylarginine, ADMA, and symmetric dimethylarginine (Gary and Clarke, 1998). Proteolytic degradation of arginine-methylated proteins results in release of free methylarginines. A recent study showed that the

This study was supported in part by the National Institutes of Health [Grants HL63080, HL68688] (to S.L.); the National Institutes of Health [Grants S10RR023461–01, NS052315–01] (to S.P.); and the American Heart Association [Grant 0555456U].

Article, publication date, and citation information can be found at http://jpet.aspetjournals.org.

doi:10.1124/jpet.109.153510.

ABBREVIATIONS: ADMA, asymmetric dimethylarginine; bp, base pair; eNOS, endothelial nitric-oxide synthase; CAT, cationic amino acid; DDAH, dimethylarginine dimethylaminohydrolase; DMSO, dimethyl sulfoxide; FXR, farnesoid X receptor; FXRE, FXR response element; BA, bile acid; RT-PCR, reverse transcription polymerase chain reaction; RXR, retinoid X receptor; UPLC, ultra performance liquid chromatography; MS, mass spectrometry; GW4064, 3-(2,6-dichlorophenyl)-4-(3'-carboxy-2-chlorostilben-4-yl)oxymethyl-5-isopropylisoxazole.

lung is a major source of methylarginines, in particular, ADMA (Bulau et al., 2007). ADMA can be degraded in situ inside cells. Nondegraded ADMA can be exported into circulation via system y^+ carriers of the cationic amino acid (CAT) family (Baylis, 2006; Palm et al., 2007). CATs are also involved in the subsequent removal of circulating ADMA by liver and kidney. Although ADMA can be excreted from the kidney, the clearance of ADMA is largely facilitated by dimethylarginine dimethylaminohydrolases (DDAHs) that are expressed as type 1 and 2 isoforms. DDAH-1 is the predominant isoform in the proximal tubules of the kidney and in the liver, and it plays a role in eliminating blood ADMA. DDAH-2 is predominantly expressed in the vasculature and may be involved in the regulation of local ADMA concentrations (Palm et al., 2007). The significance of ADMA is underscored by the fact that ADMA but not symmetric dimethylarginine acts as an inhibitor of NOS by competing with arginine, the exclusive precursor of NO. Increased levels of ADMA are associated with diminished NO production and increased ROS generation. ADMA is currently regarded as a risk factor for endothelial dysfunction, cardiovascular mortality, and progression of chronic kidney disease (Baylis, 2006; Leiper et al., 2007; Palm et al., 2007). Thus, therapeutics targeted at deceasing local or systemic ADMA may prove useful in the management of various types of cardiovascular diseases.

Several studies have shown that ligands for retinoid X receptor or estrogen receptor can promote ADMA metabolism via up-regulating DDAH-2 expression in vascular endothelial cells (Achan et al., 2002; Monsalve et al., 2007). Thus, the cardioprotective effect of estrogen may be secondary to its effect on ADMA metabolism in addition to the effects of estrogen on eNOS expression and/or activation, per se. A recent study showed that FXR may also be involved in the metabolism of ADMA (Hu et al., 2006).

FXR (NR1H4) is a member of the nuclear receptor superfamily that is highly expressed in liver, kidney, adrenals, and intestine. FXR plays a key role in the homeostasis of cholesterol and BAs via regulation of the expression of the genes that are involved in the synthesis and transport of BAs (Eloranta and Kullak-Ublick, 2005; Bertolotti et al., 2008). FXR ligands including BAs have recently been proposed as novel therapeutics in cardiovascular diseases based on their effectiveness in lowering circulating triglycerides and cholesterol, and improving hyperglycemia (Watanabe et al., 2004; Cariou et al., 2006). We, and others, have recently shown that FXR may also be directly or indirectly involved in vascular signaling (Bishop-Bailey et al., 2004; He et al., 2006; Li et al., 2008). We showed that activation of FXR in vascular endothelial cells led to up-regulation of eNOS expression and increased NO production (Li et al., 2008). Hu and colleagues recently reported that treatment of rats with a FXR ligand resulted in up-regulation of DDAH-1 expression in the liver and a concomitant decrease in the blood level of ADMA, suggesting another mechanism by which FXR affects NO signaling (Hu et al., 2006). We report in this study that treatment of mice with GW4064 induced the expression of DDAH-1 in both liver and kidney, and a significant decrease in the blood level of ADMA. Moreover, activation of FXR also induced CAT-1 in intact mouse liver and kidney and in cultured human liver and kidney cells, suggesting a comprehensive role for FXR in regulating ADMA homeostasis.

Materials and Methods

Drugs and Chemical Reagents. ADMA (as the hydrochloride salt) was purchased from Sigma-Aldrich (St. Louis, MO). GW4064 and deuterated ADMA ($^2H_6$-ADMA) were synthesized according to published protocols, respectively (Maloney et al., 2000; Martens-Lobenhoffer et al., 2004). All products for cell culture were purchased from Invitrogen (Carlsbad, CA). pCMX, pCMX-FXR, and pCMV-βgal were described previously (He et al., 2006). pCMX-vpFXR (a gift from Drs. Enrique Saez and Ronald Evans at the Salk Institute) was generated by fusing the VP16 activation domain from the herpes simplex virus to the N terminus of the FXR. pCMX-FXR-DN, a plasmid expressing a dominant negative rat FXR (an AF-2 domain deletion mutant), was constructed according to a published protocol (Kocarek et al., 2002).

Cell Culture. Human proximal tubular epithelial cells (HKC-8) were kindly provided by Dr. Lorraine Racusen at Johns Hopkins University School of Medicine. HKC-8 cells were cultured in Dulbecco's modified Eagle's medium/F-12 medium supplemented with 10% fetal bovine serum. The African green monkey kidney cell line CV-1 and human hepatoma cell line HepG2 were obtained from American Type Culture Collection (Manassas, VA) and were cultured in Dulbecco's modified Eagle's medium supplemented with 10% fetal bovine serum, 0.1 mM nonessential amino acids, 1 mM sodium pyruvate, streptomycin (100 μg/ml), and penicillin (100 U/ml).

Animal Care and Treatment. Male C57BL/6 mice (Charles River Laboratories, Wilmington, MA) weighing between 18 and 20 g were used in all experiments. FXR ligand GW4064 or vehicle control (sesame oil) was given by single daily instillation via gavages for 5 consecutive days at a dose of 25, 50, or 100 mg/kg in 50 μl of sesame oil. Four hours after the last dosage, blood samples were collected from the periorbital sinus into tubes coated with heparin while the mice were under general anesthesia with isoflurane. The mice were then asphyxiated with carbon dioxide; the organs were harvested, quickly frozen on dry ice, and stored at −70°C.

DDAH Activity Measurement. DDAH activity was measured by the conversion of ADMA to L-citrulline (Tain and Baylis, 2007). In brief, protein concentration was determined by the BCA Protein Assay (Pierce Chemical, Rockford, IL) and adjusted to 20 mg/ml. The protein homogenate was preincubated with urease to eliminate interference of the analysis by urea. To 100 μl of this protein sample, 400 μl of 1 mM ADMA in sodium phosphate buffer was added and incubated at 37°C for 45 min. The reaction was stopped by addition of 4% sulfosalicylic acid. Samples were then mixed and centrifuged. A 100-μl aliquot of supernatant was mixed with 100 μl of color reagent (one part 0.8% oxime reagent to two parts 0.5% antipyrine reagent) and allowed to react for 1.5 h at 60°C in the dark. Standards were prepared by use of 3 to 50 mM L-citrulline. The absorption was read spectrophotometrically at 450 nm. DDAH activity is presented as millimolar L-citrulline per gram of protein per minute at 37°C. All activity measurements were performed in triplicate.

Nitrite/Nitrate Assays. Blood was collected in the presence of the anticoagulant EDTA (Vacutainer; BD, Franklin Lakes, NJ), and plasma was separated by centrifugation. The plasma samples were filtered through a 10-kDa molecular mass cutoff filter (Microcon; Millipore Corporation, Billerica, MA). Plasma NO was determined by measuring nitrate and nitrite by use of a nitrate/nitrite colorimetric assay kit (Cayman Chemical, Ann Arbor, MI). In brief, samples were incubated with nitrate reductase and NADPH cofactor for 3 h to convert nitrate into nitrite. The total amount of NO was then determined by use of the Griess reagent. A standard curve was determined by use of known concentrations of nitrate assayed at 550 nm with a microplate reader. The NO concentrations in samples were calculated by use of the standard curve. The results were expressed as micromolar nitrate/nitrite.

ADMA Uptake. Uptake of ADMA by HKC-8 or HepG2 cells was determined with UPLC-MS measurements. The cells were grown to 70 to 80% confluence in 100-mm dishes. Before uptake studies, the

cells received treatments of GW4064 or vehicle (DMSO) alone for 18 h. The cells were washed three times in HEPES-Krebs and incubated at 37°C for 30 min in serum-free medium containing the DDAH inhibitor *S*-nitroso-L-homocysteine (800 mM) that was synthesized according to the method of Stamler and Feelisch (1996). The cells were then treated with $^2H_6$-ADMA (10 μM) in HEPES-Krebs buffer for 20 min. After treatment cells were washed with ice-cold phosphate-buffered saline and lysed with 500 μl of lysate buffer. Cell lysates were centrifuged, and the supernatant was extracted by use of a Microcon centrifugal filter cartridge (10,000 nominal molecular weight limits; Millipore Corporation) after addition of 10 μl of 5 mM ADMA solution as internal standard. The sample was diluted by adding 100 μl of a mixture of acetonitrile/formic acid (100:0.01, v/v). Protein concentration was determined by the BCA protein assay before extraction of the supernatant. $^2H_6$-ADMA levels were determined by liquid chromatography-tandem mass spectrometry/mass spectrometry as described below with a five-point calibration curve of $^2H_6$-ADMA standards (0.5–10 mM). ADMA uptake is reported as millimolar $^2H_6$-ADMA per milligram of protein.

ADMA Measurement in Serum. For the UPLC separation, a Waters Acquity UPLC system (Milford, MA) was used with a Waters UPLC BEH C18 analytical column (1.7 mm, 2.1 × 100 mm). The analytes were detected by a TSQ Quantum Ultra triple quadrupole mass spectrometer equipped with an electrospray ion source (Thermo Fisher Scientific, Waltham, MA). Instrument control, data collection, and analysis were performed by the Thermo Xcalibur software package (Thermo Fisher Scientific). Twenty microliters of the internal standard solution (9 mM $^2H_6$-ADMA in water) was added to 100 μl of serum. The sample was diluted by adding 100 μl of a mixture of acetonitrile/formic acid (100:0.01, v/v) and applied to a Microcon centrifugal filter cartridge (10,000 NMWL; Millipore Corporation). After centrifugation at 14,000*g* for 30 min at ambient temperature, a 3-μl volume of the sample was injected into the UPLC system. The chromatographic separation was achieved by gradient elution: mobile phase A = 100% water and 0.1% formic acid; and mobile phase B = 100% acetonitrile and 0.1% formic acid at a flow rate of 0.3 ml/min with 100% A for 2 min and linear increase to 70% B over 3 min with subsequent equilibration with 100% A for 1 min. In the mass spectrometer, the analytes were ionized by an electrospray ion source, working in the positive mode. For all analytes, molecular ions in the form [M + H]+ were produced. No source fragmentation products, dimers, or adduct ions were observed. After fragmentation with argon as collision gas, the specific fragment ions *m/z* 203→46 for ADMA and *m/z* 209→70 for $^2H_6$-ADMA. A stock solution of ADMA (3 mmol in 100 ml of water) was used to make standards in serum or water for a five-point calibration curve of 0.2 to 3 mM. The peak area ratios of analyte/internal standard were used for quantification.

Quantitative Real-Time RT-PCR Assay of CAT-1 and DDAH-1 mRNA Expression. Total RNA was extracted from tissues or cells with TRIzol reagent (Invitrogen) and the first-strand cDNA was synthesized by use of SuperScript III reverse transcriptase (Invitrogen). Real-time PCR analysis of mouse or human DDAH-1 or CAT-1 was performed by use of SYBR Green-based assays with the ABI 7300 Real-Time PCR System (Applied Biosystems, Foster City, CA). Each amplification mixture (25 μl) contains 25 ng of cDNA, 1.25 μl of primers and FAM-labeled florigenic probe, and 12.5 μl of Universal PCR Master mix. Amplification was performed under the following conditions: 50°C for 2 min, 95°C for 10 min, and 40 cycles of 95°C for 15 s, and 60°C for 1 min. Transcript abundance, normalized to β-glucuronidase expression, was expressed as fold increase over a calibrated sample.

Western Blot Analysis for CAT-1 Protein Expression. Protein extraction and Western blot analysis were performed as described previously (Li et al., 2008). Goat anti-CAT-1 antibody (C-12) was purchased from Santa Cruz Biotechnology, Inc. (Santa Cruz, CA). Horseradish peroxidase-labeled sheep anti-goat IgG and the electrochemiluminescence kit were purchased from GE Healthcare (Piscataway, NJ).

Transfection Assays. Normal monkey kidney fibroblast cells (CV-1 line) were grown to 60 to 70% confluence in 48-well plates. Cells were transiently transfected with Lipofectamine 2000 (Invitrogen) with pGL3-CAT-1 in the presence or absence of pCMX-vpFXR or pCMX-FXR. pCMX was added to ensure that amounts of DNA in each well were identical. Transfection efficiency was monitored by cotransfection of pCMV-βgal plasmid. Cell extracts were prepared after transfection, the luciferase and β-galactosidase assays were performed as described previously (He et al., 2006), and luciferase activity was normalized against β-galactosidase activity. Transfection experiments were performed on at least three occasions and in each case were done in triplicate. Data were represented as fold induction over reporter gene alone.

Electrophoretic Mobility Shift Assay. FXR and retinoid X receptor (RXR) proteins were generated in vitro by coupled transcription/translation (TNT system; Promega, Madison, WI) with pCMX-FXR and pCMX-RXR plasmids. The DNA probe CAT-1/IR0 (5′-aag**gggtcatgacc**actgg-3′) was derived from a region in the rat CAT-1 promoter that contains a putative FXR response element (bold). It was labeled with [γ-^{32}P]ATP by using the Klenow fragment of DNA polymerase. DNA-binding reactions were performed as follows. Aliquots of in vitro translation mixture were incubated in 20 μl of binding buffer (10 mM HEPES, pH 7.9, 10 mM EGTA, 10 mM EDTA, 0.25 mM dithiothreitol, and 10% glycerol) containing 2 μg poly(dI:dC) (Sigma-Aldrich) and 6 to 20 × 10^3 cpm of DNA probe at room temperature for 20 min. For supershift assays, 0.2 μg of rabbit anti-FXR IgG was added, and the samples were incubated for another 10 min. The binding mixture was then applied to a 5% polyacrylamide gel (0.5× TrisBorateEDTA buffer) for electrophoresis. The gels were dried and exposed at −80°C for autoradiography.

Statistical Analysis. All data are expressed as means ± S.E.M. unless otherwise stated. Comparisons between two groups were made with unpaired Student's *t* test. Comparisons between three or more groups were made with analysis of variance followed by Tukey-Kramer post hoc analysis. In all cases, $P < 0.05$ was considered statistically significant.

Results

GW4064 Treatment Results in Decreased Plasma Concentrations of ADMA and Increased NO Production in Mice. Figure 1A shows that oral administration of GW4064 in mice resulted in a significant decrease in plasma level of ADMA at three different doses (25, 50, and 100 mg/kg) tested. These results were consistent with a previous report by Hu and colleagues, in which GW4064 treatment decreased plasma ADMA level in rats (Hu et al., 2006). It seems that there was a trend of increase in ADMA concentration as the GW4064 dosage increased from 25 to 100 mg/kg (Fig. 1A). It remains to be investigated if this trend is caused by some specific effects of GW4064 at a relatively high dose. GW4064 treatment also led to increased NO production in mice as shown by increased levels of nitrates/nitrites in the plasma (Fig. 1B).

GW4064 Treatment Results in Up-regulation of DDAH-1 Expression and Increases in DDAH Activities in Mouse Liver and Kidney. Liver and kidney play an important role in regulating circulating ADMA concentrations through DDAH-mediated degradation. The study by Hu et al. (2006) showed that GW4064 treatment led to up-regulation of DDAH-1 expression in rat liver, which might contribute to the decreased ADMA concentrations in the circulation. A similar result was observed in our study: GW4064 treatment led to increased expression of DDAH-1 mRNA in mouse liver (Fig. 2A). Up-regulation of DDAH-1 expression was associated with an increased DDAH activity in the liver

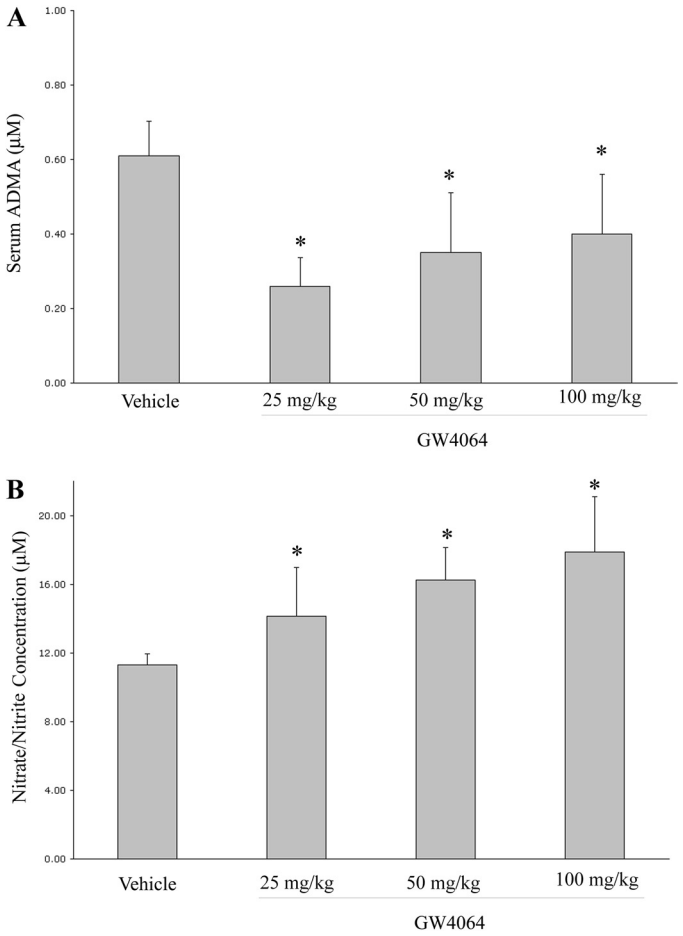

Fig. 1. Oral GW4064 treatment led to decreased plasma ADMA concentrations (A) and increased plasma levels of nitrite/nitrate (B) in mice. Male C57BL/6 mice received daily gavage of GW4064 for 5 days at a dose of 25, 50, or 100 mg/kg. Control mice were treated with vehicle alone (sesame oil). Plasma samples were prepared 4 h after the last dose and subjected to ADMA and nitrite/nitrate analysis as detailed under *Materials and Methods*. *, $P < 0.05$ (versus sesame oil alone). $n = 7$.

(Fig. 2B). GW4064 treatment similarly led to increased expression of DDAH-1 and enhanced DDAH activities in mouse kidney (Fig. 2, A and B). Induction of DDAH-1 was also observed in human hepatoma cells (HepG2) and human proximal tubular epithelial cells (HKC-8) (Fig. 3A). This finding was associated with a significant increase in DDAH activities in the treated cells (Fig. 3B). However, the magnitude of increase in activity is relatively small compared with the fold of induction at the levels of mRNA and proteins. This might be due to, among other things, a relatively high nonspecific background. This will be addressed further in the future.

GW4064 Treatment Leads to Up-regulation of CAT-1 in Mouse Liver and Kidney. In addition to DDAH, CAT also plays an important role in ADMA homeostasis via its involvement in both exports of ADMA from cells/tissues into the circulation and its subsequent uptake from the blood by liver and kidney for metabolism. Therefore, we further examined the effect of GW4064 on CAT-1 expression in mouse liver and kidney. Figure 4 shows that there was a significant induction of CAT-1 in liver at both mRNA (A) and protein (B) levels after GW4064 treatment. GW4064 treatment similarly induced CAT-1 expression in mouse kidney (Fig. 4, A and B). CAT-1 up-regulation was also demonstrated in cultured human kidney proximal tubular epithelial cells (HKC-8) and hepatoma cells (HepG2) at both mRNA (Fig. 5A) and protein (Fig. 5B) levels. To study the role of CAT-1 up-regulation in ADMA uptake, we then examined the effect of GW4064 on the uptake of deuterated ADMA by either HKC-8 or HepG2 cells. The amount of deuterated ADMA that is taken up by cells was determined by UPLC-MS. As shown in Fig. 5C, GW4064 treatment led to a significant increase in the uptake of deuterated ADMA by HKC-8 cells. A similar result was shown in the cultured HepG2 cells (Fig. 5C).

FXR Enhances Transcriptional Activation of the Rat CAT-1 Gene Promoter. To examine whether GW4064-mediated increases in the levels of CAT-1 mRNA are due to an enhancement in gene transcription or an increased mRNA stability, CAT-1 mRNA abundance was similarly examined in HepG2 cells that were treated with a transcription inhibitor, actinomycin D, before GW4064 treatment. As shown in Fig. 6A, pretreatment with actinomycin D substantially inhibited GW4064-mediated up-regulation of CAT-1 mRNA, suggesting that GW4064 enhanced CAT-1 mRNA expression in HepG2 cells at the transcriptional level. A similar result was shown in HKC-8 cells (Fig. 6B).

CAT-1 Is a Probable Transcriptional Target of FXR. To further examine whether CAT-1 promoter is a transcriptional target of FXR, we constructed several luciferase reporter expression plasmids (pGL3-CAT-1) that are driven by up to 1.5-kb sequences of rat CAT-1 promoter. CV-1 cells were transfected with pGL3-CAT-1-1.5kb in the absence or presence of a FXR expression vector. As shown in Fig. 7A, treatment with GW4064 alone resulted in a slight increase in the transcriptional activity of the 1500-bp CAT-1 promoter. This might be due to a low level of endogenous FXR activity in CV-1 cells. Such an increase in CAT-1 promoter activity was more pronounced when the cells were cotransfected with a FXR expression plasmid. The increases in promoter activity were substantially abolished when CV-1 cells were cotransfected with a dominant-negative FXR (D/N FXR) expression plasmid, suggesting that GW4064 enhances CAT-1 promoter activity largely via activation of FXR. To further elucidate a role of FXR in regulating CAT-1 promoter activity, we then cotransfected pGL3-CAT-1 with an expression plasmid encoding a constitutively activated FXR, vpFXR. pCMX-vpFXR was generated by fusing the VP16 activation domain from the herpes simplex virus to the N terminus of the FXR cDNA. Figure 7A shows that coexpression of vpFXR in CV-1 cells significantly enhanced the CAT-1 promoter activity, clearly demonstrating that a genetic activation of FXR enhances CAT-1 promoter activity. Similar results were observed in transfection with a luciferase reporter driven by a shorter rat CAT-1 promoter (~470 bp) (Fig. 7B). However, further deletion of CAT-1 promoter to 390 bp resulted in a drastic decrease in the promoter activity (Fig. 7C), suggesting a probable presence of a FXR response element (FXRE) in the 80-bp promoter region (−390 to −470).

To search for FXREs that may mediate CAT-1 induction by GW4064, the 470-bp CAT-1 promoter sequence was subjected to in silico analysis with a Web-based algorithm NUBIScan (Podvinec et al., 2002). One such potential FXRE was identified, and its sequence and location are shown in Fig. 8A. There is a hexameric core sequence GGGTCA between −409 and −404. This is followed by a perfect inverted repeat sequence TGACCC (−403 to −398). This forms a perfect in-

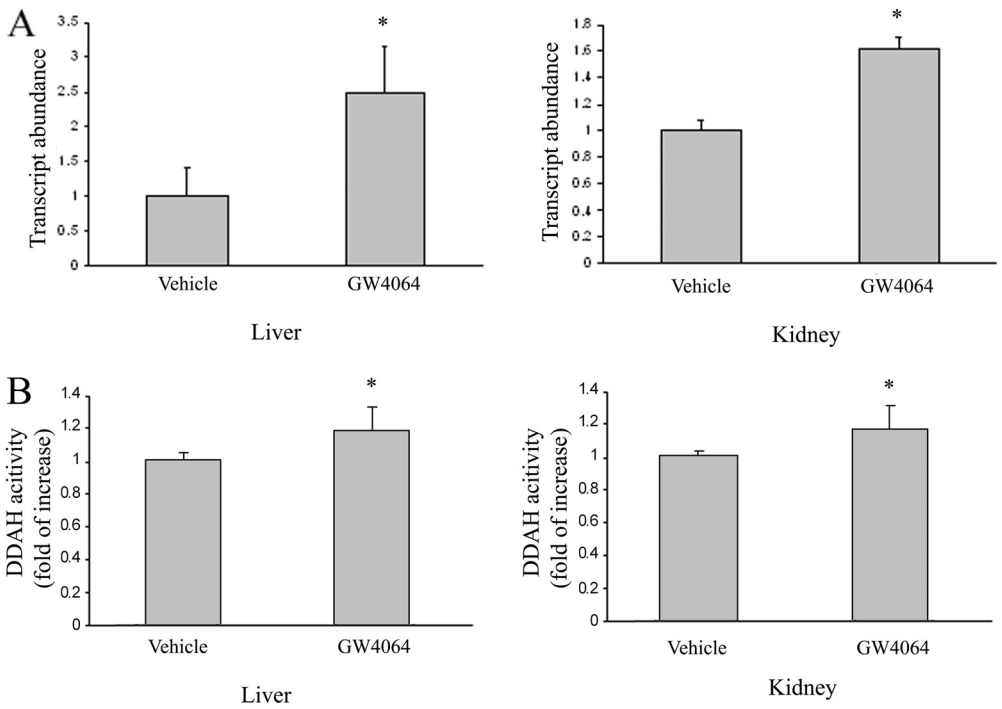

Fig. 2. Oral GW4064 treatment led to up-regulation of DDAH-1 in mouse liver and kidney. Mice received GW4064 or vehicle treatment as described in the legend to Fig. 1. Four hours after the last dose, mice were sacrificed, and livers and kidneys were collected. A, DDAH-1 expression in the tissues was examined by real-time RT-PCR. B, DDAH activity in the tissues was also determined by a colorimetric assay. $n = 4$.

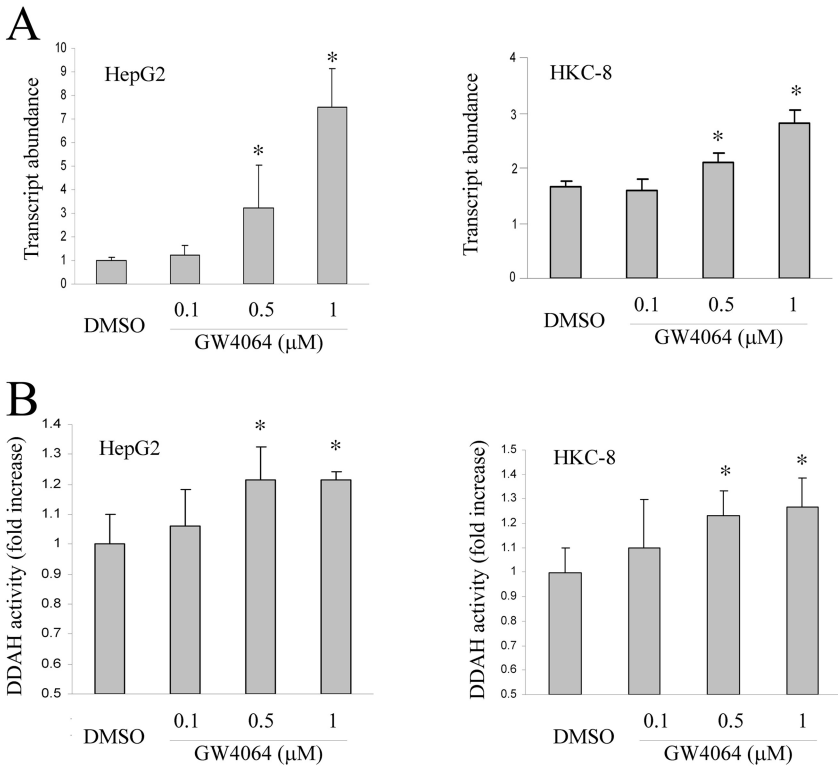

Fig. 3. GW4064 treatment led to up-regulation of DDAH-1 mRNA expression and increased DDAH activity in human hepatoma cells (HepG2) and human proximal tubular epithelial cells (HKC-8). HepG2 or HKC-8 cells were treated with DMSO or various concentrations of GW4064. DDAH-1 mRNA expression (A) and DDAH activity (B) in the cells were determined 24 h later as described in the legend to Fig. 2. $n = 3$.

verted repeat motif IR0 (-gggtcatgaccc-), a type of nuclear receptor response element that has been shown to be used by FXR (Echchgadda et al., 2004). To determine whether this IR0 sequence is responsible for FXR-mediated transactivation of CAT-1 promoter, we generated a pGL3-CAT-1 in which this putative FXR binding site was mutated. The wild-type and mutated plasmids were then similarly subjected to transfection in CV-1 cells, and their transfection efficiency was compared. Figure 8B shows that the FXR-mediated activation of CAT-1 promoter (−470 bp) was substantially diminished when the CAT-1/IR0 site was disrupted, further suggesting a role of this IR0 site in FXR-mediated transactivation of rat CAT-1 promoter.

To determine whether FXR directly binds to this element, electrophoretic mobility shift assays were performed with a 20-bp oligonucleotide that contains the CAT-1/IR0. A typical IR1/FXRE oligonucleotide was also included as a positive control, because FXR is known to bind to IR1 with high specificity and affinity. Interaction of CAT-1/IR0 oligonucleotide with in vitro translated FXR/RXR yielded a DNA/pro-

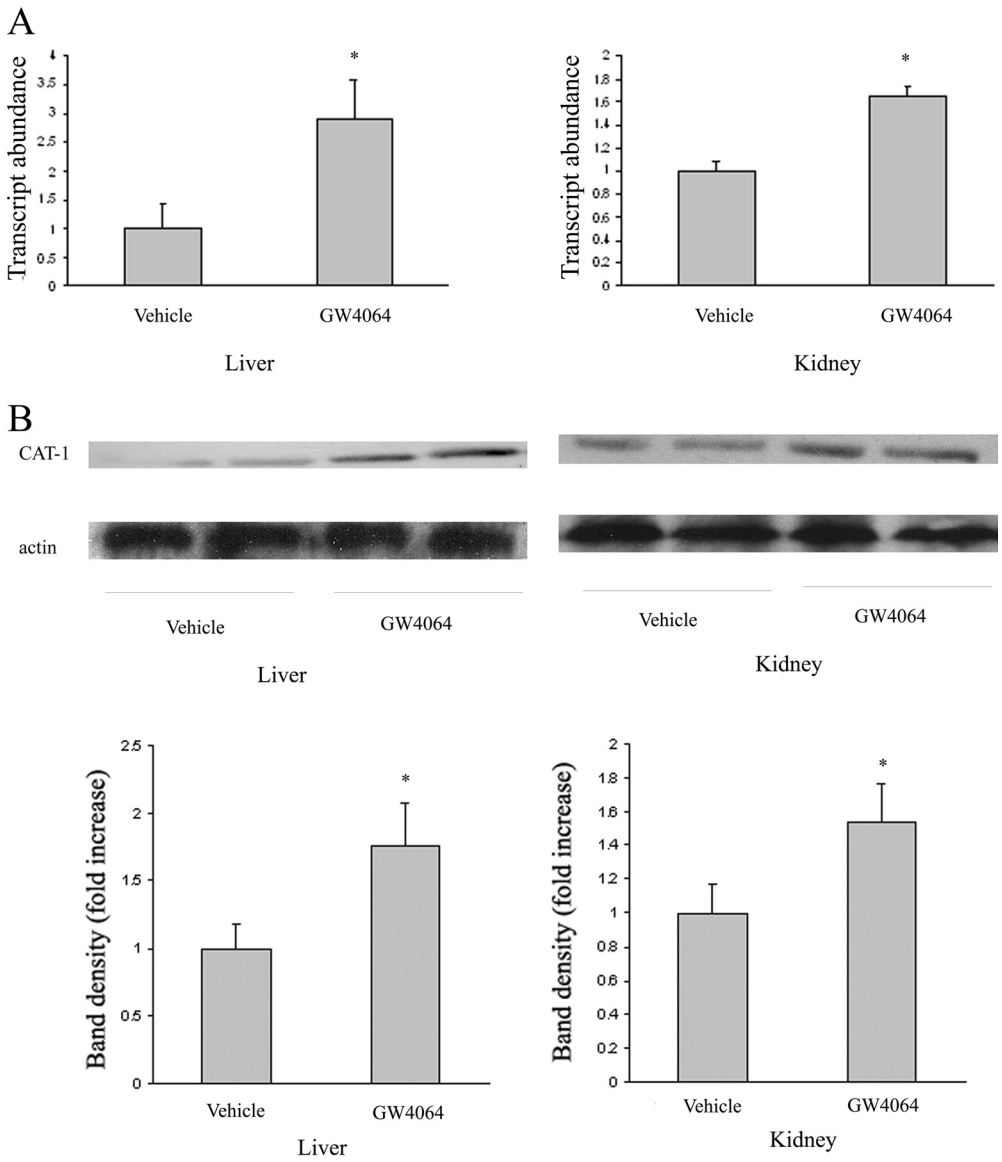

Fig. 4. Oral GW4064 treatment led to up-regulation of CAT-1 in mouse liver and kidney. Mice received GW4064 or vehicle treatment as described in the legend to Fig. 1. Four hours after the last dose, mice were sacrificed, and livers and kidneys were collected. CAT-1 expression in the tissues was examined by real-time RT-PCR (A) and Western blot analysis (B), respectively. $n = 6$.

tein band of expected mobility (Fig. 8C). This binding was specific, because it was inhibited by addition of excess unlabeled (cold) CAT-1/IR0 or IR1/FXRE (Fig. 8C). Addition of antibody against FXR to the reaction mixture resulted in further retarded migration of the radiolabeled band (Fig. 8C). This supershifting confirms the identity of the protein that interacts with the DNA as being FXR. These results strongly suggest that CAT-1/IR0 is likely to mediate the transactivation of CAT-1 promoter by FXR.

Discussion

We have shown in this study that CAT-1 is a novel FXR target gene. We have also shown that GW4064 induced the expression and activity of DDAH-1 in the liver and kidney. Our study confirmed and expanded the observation made by Hu et al. (2006) in rats. The regulation of CAT-1 and DDAH-1 by FXR was conserved in human cells. We propose that the combined effect of FXR on the expression of CAT-1 and DDAH-1 in the liver and kidney may account for the ADMA-lowering effect of GW4064.

The role of DDAH in ADMA metabolism has been well established in studies in DDAH transgenic and/or knockout mice. It has been shown that DDAH-1 is largely located in the liver and kidney and plays a role in eliminating blood ADMA, whereas DDAH-2 is predominantly expressed in the vasculature and may be involved in the regulation of local ADMA concentrations (Palm et al., 2007). However, DDAH-2 transgenic mice also show lower blood levels of ADMA compared with wild-type mice. This might be due to increased ADMA metabolism inside the tissues and therefore decreased export of ADMA to the circulation (Hasegawa et al., 2007). In addition to induction of DDAH-1 expression in liver and kidney, our preliminary studies also showed increased expression of DDAH-2 in GW4064-treated mouse lungs (Li Jiang et al., unpublished results). A study by Bulau et al. (2007) suggests that lungs are a major source of ADMA in mice: the lungs expressed significantly higher levels of PRMT1, PRMT2, and PRMT6 compared with the heart, kidney, or liver, and arginine residues in lung protein hydrolysates exhibited a 4-fold higher degree of asymmetrical and 2-fold higher degree of symmetrical dimethylation compared with arginine residues from heart, kidney, and liver tissue.

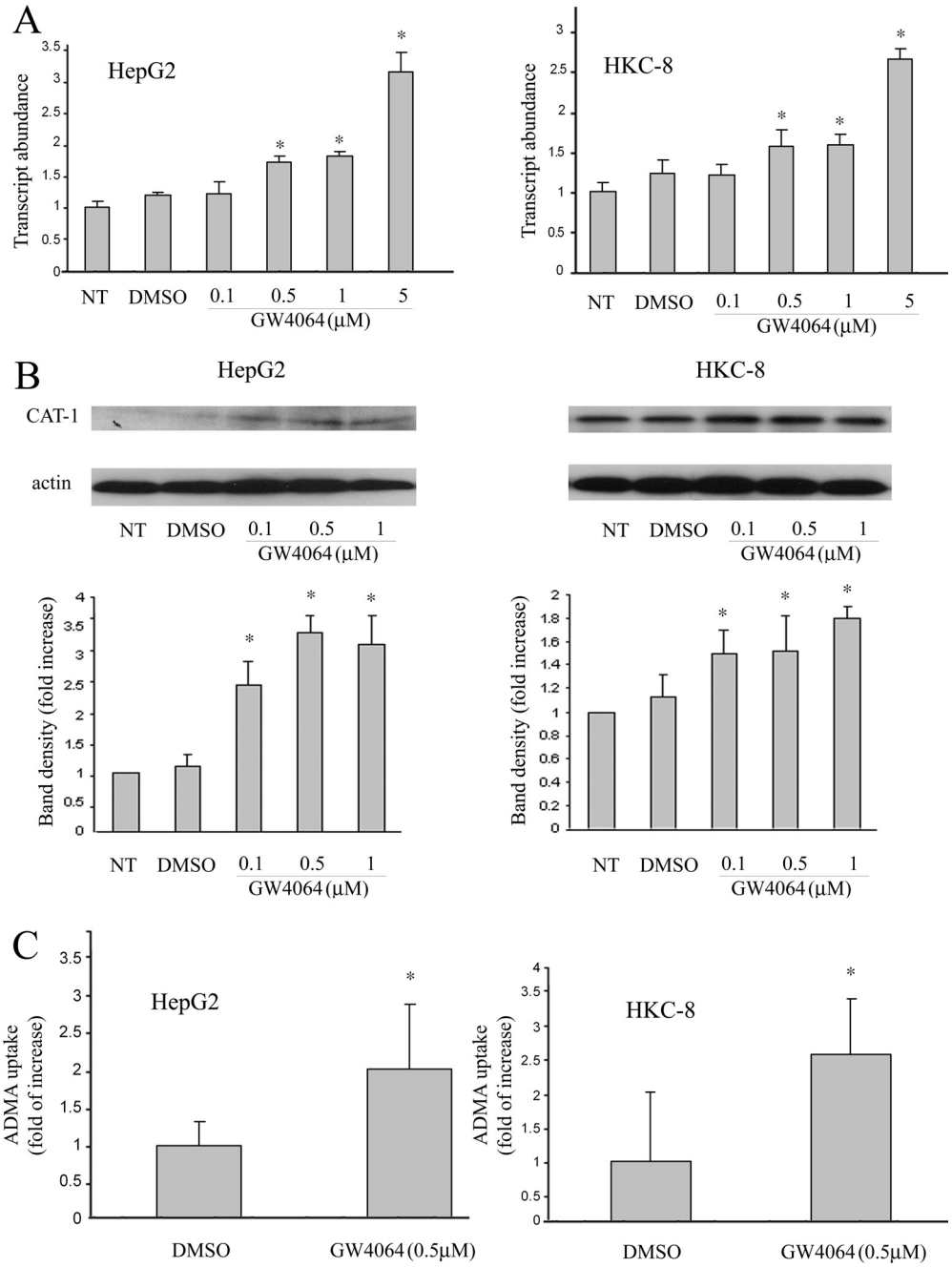

Fig. 5. GW4064 treatment led to upregulation of CAT-1 expression in cultured human proximal tubular epithelial cells (HKC-8) and human hepatoma cells (HepG2), and increased cellular uptake of ADMA. HKC-8 or HepG2 cells at 70% confluence were treated with various concentrations of GW4064 or vehicle alone (DMSO). The expression of CAT-1 mRNA (A) and protein (B) was examined at 16 and 24 h after the treatment by real-time RT-PCR and Western blot analysis, respectively. In a separate experiment, cells were similarly treated with GW4064 or DMSO for 18 h. Cells were then treated with $^2H_6$-ADMA (10 μM) in HEPES-Krebs buffer for 20 min. C, the amounts of $^2H_6$-ADMA that are taken up by cells were determined by UPLC-MS as described under *Materials and Methods*. $n = 6$. NT, no treatment.

Thus, the increased DDAH-2 expression in the lungs may also contribute to the decreased plasma ADMA concentration in GW4064-treated mice. This will be addressed further in the future.

CAT has previously been studied extensively for their roles in the transport of arginine, the substrate for NO synthase (Hatzoglou et al., 2004). Altered CAT expression has been implicated in a number of pathological conditions such as congestive heart failure and acute and chronic renal failure (Reade et al., 2002). Recent studies showed that CAT is also involved in both cellular release and uptake of ADMA and may play an important role in intercellular and interorgan transport of ADMA (Teerlink, 2005). It has been well documented that plasma ADMA concentrations are elevated in the patients with advanced cardiovascular, liver, and renal diseases (Kielstein and Zoccali, 2008; Wilson et al., 2008). Most studies attributed the decreased DDAH activity in the affected organs to the increased blood levels of ADMA. Considering the important role of CAT in the clearance of ADMA, it is likely that the altered CAT-1 expression may also contribute to the increases in the blood levels of ADMA.

The regulation of CAT-1 has been studied extensively (Mann et al., 2003; Hatzoglou et al., 2004). In response to situations such as nutritional stress and immune activation, CAT-1 activity can be regulated at transcriptional, post-transcriptional, or post-translational level. It has been suggested that induction of CAT-1 in the liver by insulin plays an important role in modulation of blood levels of ADMA and contributes to the beneficial effects found in critically ill patients receiving intensive insulin therapy (Siroen et al., 2005). However, little is known about

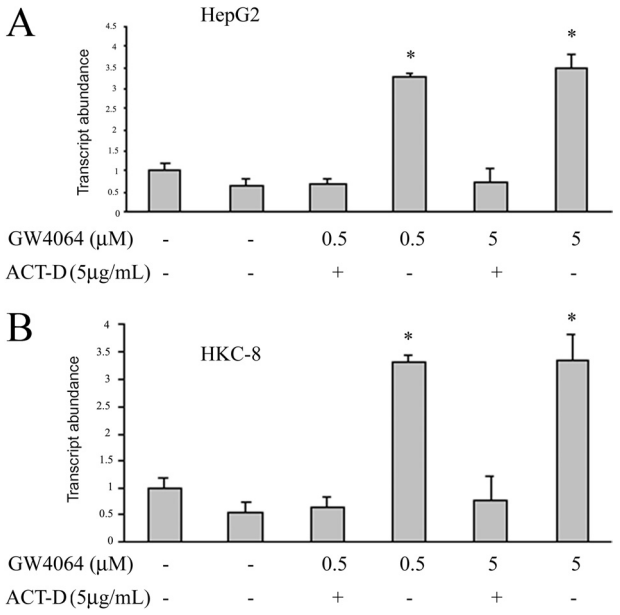

Fig. 6. Treatment with actinomycin D abolished GW4064-mediated up-regulation of CAT-1 mRNA expression. HepG2 (A) or HKC-8 (B) cells were treated with actinomycin D (5 μg/ml) for 30 min before GW4064 treatment. Eighteen hours later, CAT-1 mRNA expression in the cells was similarly examined by real-time RT-PCR as described in the legend to Fig. 5. ACT-D, actinomycin D.

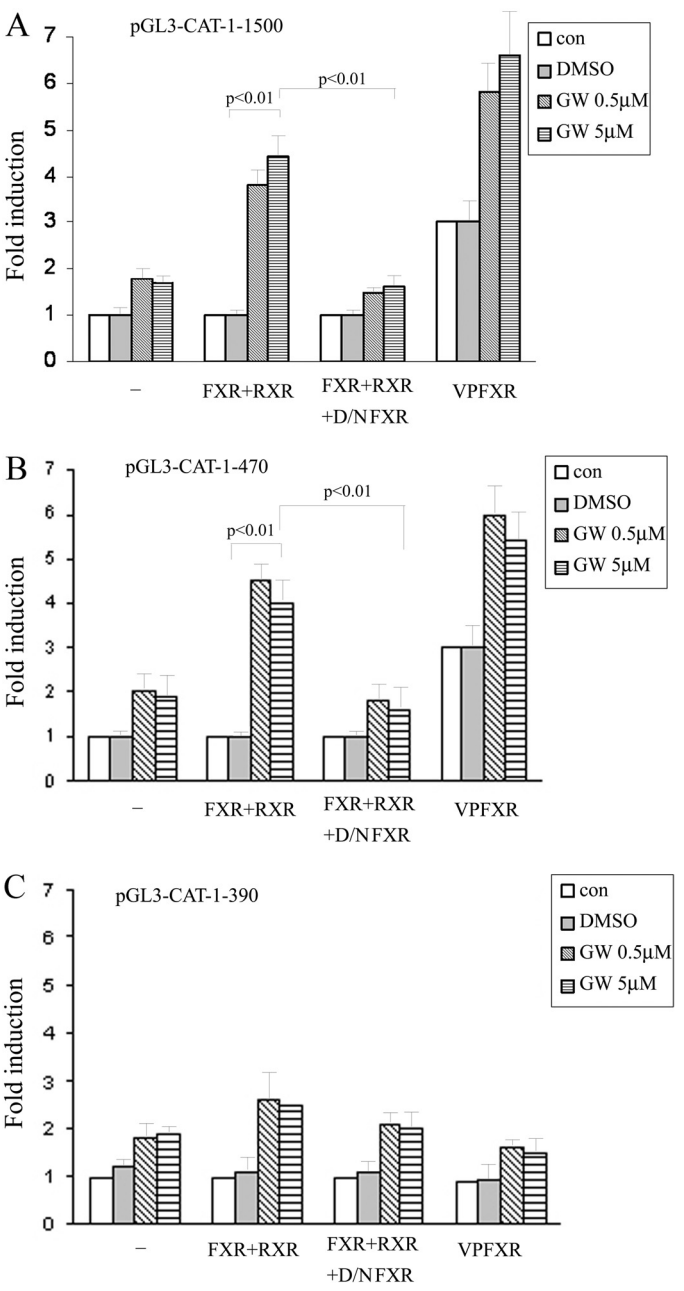

Fig. 7. FXR enhances the transcriptional activity of the CAT-1 gene promoter. A luciferase reporter driven by a rat CAT-1 promoter of 1500 bp (A), 470 bp (B), or 390 bp (C) was used to study the CAT-1 promoter activity. CV-1 cells were transiently transfected with pGL3-CAT-1 in the presence or absence of pCMX-FXR. Five hours later, the transfection medium was replaced with complete medium and cells were incubated for 12 h. Cells were then cultured in the presence of GW4064 or vehicle DMSO for 24 h. Luciferase assay was then performed. The data shown represent the mean (S.D.) from triplicate assays. In some studies, cells were cotransfected with pCMX-FXR and pCMX-FXR-DN at a weight ratio of 1:2. Luciferase assay was then similarly performed. To examine the effect of genetic activation of FXR on CAT-1 promoter activity, CV-1 cells were transfected with pGL3-CAT-1 in the presence or absence of pCMX-vpFXR. Luciferase assays were then examined as described.

roles of nuclear receptors in the regulation of CAT-1 expression. Our data suggest that GW4064 treatment led to significant up-regulation of CAT-1 in mouse kidney and liver. A similar result was shown in cultured human kidney epithelial cells and hepatoma cells. Such up-regulation was associated with a significant increase in uptake of ADMA in these cultured cells. FXR seems to regulate CAT-1 expression at transcriptional level because the ligand-mediated increase in the expression of CAT-1 mRNA was substantially abolished by actinomycin D, and CAT-1 promoter activity was significantly increased via pharmacological or genetic activation of FXR. Furthermore, we have identified an IR0 as the FXRE that seems to be involved in GW4064-mediated up-regulation of CAT-1 in kidney or liver cells. It has been shown that FXR/RXR can bind to and activate a variety of elements, including IR1 elements with changes in the core half-site sequence, spacing nucleotide, and flanking nucleotides, although FXR/RXR binds to the consensus IR1 sequence with the highest affinity (Jung et al., 2006). For example, IR0, IR2, IR8, and ER8 have been shown to be capable of conferring responsiveness on several FXR-target genes (Anisfeld et al., 2005; Li et al., 2008). It remains to be examined whether the IR0-mediated FXR transactivation of CAT-1 promoter is species-specific.

We have previously shown that FXR ligands induce up-regulation of eNOS expression and enhance NO production in vascular endothelial cells (Li et al., 2008). These, together with the data from this study, suggest a likely role of FXR in NO signaling via regulating several target genes in multiple organs. It is interesting to note that FXR ligands have recently been proposed as a new therapeutics in cardiovascular diseases based on their effectiveness in lowering circulating triglycerides and cholesterol, and improving hyperglycemia (Watanabe et al., 2004; Cariou et al., 2006). In light of the important role of NO in lipid and glucose metabolism, it will be interesting to examine whether FXR/NO signaling also contributes to the FXR-mediated antidiabetic and antihyperlipidemic effects. Despite the demonstrated beneficial effect of FXR/FXR ligands, FXR activation is also associated with some adverse effects such as decreases in the blood levels of high-density lipoprotein, induction of ICAM-1 expression in hepatocytes, and so on (Cariou and Staels, 2007). Future

A

Binding site	Core sequence
IR1 (consensus)	AGGTCA n TGACCT
rDDAH1	GGGTCA a TGACCA
CAT-1 IR0	GGGTCATGACCC
Mutated IR0	AGTGCAAGATCT

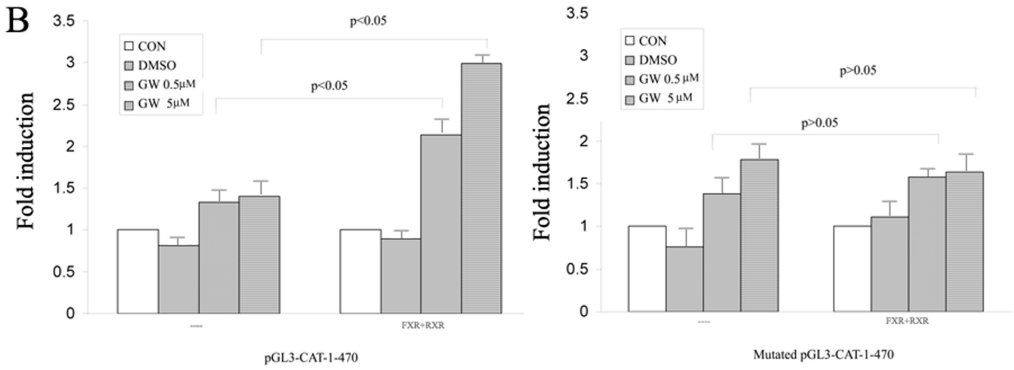

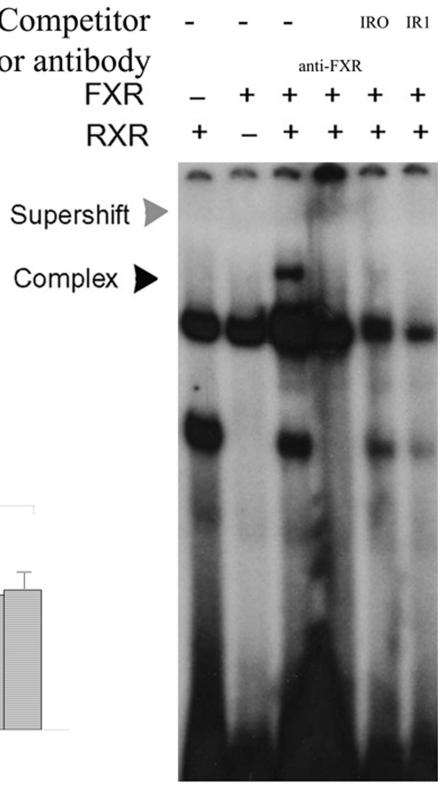

Fig. 8. Analysis of putative FXREs in rat CAT-1 promoter. A, identification of a putative FXRE in rat CAT-1 promoter via an in silico analysis with a Web-based algorithm (NUBIScan). B, mutation of IR0 on the CAT-1 promoter eliminates activation by FXR. C, electrophoretic mobility shift assay analysis of the binding of FXR/RXR to IR0 in rat CAT-1 promoter. Double-stranded oligonucleotides (–aag**gggtcatgaccc**actgg/–ccagtgggtcatgacccctt) were end-labeled with [γ-^{32}P]ATP using T4 polynucleotide kinase. The labeled probe was incubated with in vitro-translated RXR/FXR for 20 min. The reactions were analyzed by electrophoresis in a nondenaturing 5% polyacrylamide gel followed by autoradiography. In some studies, the samples were preincubated with anti-FXR antibody before gel electrophoresis. —, control.

directions in the development of FXR ligands-based therapy are likely to include selective BA receptor modulators that selectively regulate the expression of a subset of FXR target genes (Cariou and Staels, 2007).

In summary, we have shown in this study that GW4064 treatment led to coordinated up-regulation of DDAH-1 and CAT-1 in mouse liver and kidney. In addition, our results suggest that CAT-1/IR0 is likely to mediate the transactivation of CAT-1 promoter by FXR. More studies on the roles of FXR/DDAH-1/CAT in ADMA metabolism will further establish FXR as a regulator of NO signaling via the modulation of several target genes in multiple organs.

Acknowledgments

We thank Megan Klamerus and Patrick Oberly for assistance with ADMA determination.

References

Achan V, Tran CT, Arrigoni F, Whitley GS, Leiper JM, and Vallance P (2002) *all-trans*-Retinoic acid increases nitric oxide synthesis by endothelial cells: a role for the induction of dimethylarginine dimethylaminohydrolase. *Circ Res* **90:**764–769.

Anisfeld AM, Kast-Woelbern HR, Lee H, Zhang Y, Lee FY, and Edwards PA (2005) Activation of the nuclear receptor FXR induces fibrinogen expression: a new role for bile acid signaling. *J Lipid Res* **46:**458–468.

Baylis C (2006) Arginine, arginine analogs and nitric oxide production in chronic kidney disease. *Nat Clin Pract Nephrol* **2:**209–220.

Bertolotti M, Gabbi C, Anzivino C, Carulli L, Loria P, and Carulli N (2008) Nuclear receptors as potential molecular targets in cholesterol accumulation conditions: insights from evidence on hepatic cholesterol degradation and gallstone disease in humans. *Curr Med Chem* **15:**2271–2284.

Bishop-Bailey D, Walsh DT, and Warner TD (2004) Expression and activation of the farnesoid X receptor in the vasculature. *Proc Natl Acad Sci U S A* **101:**3668–3673.

Böger RH (2003) The emerging role of asymmetric dimethylarginine as a novel cardiovascular risk factor. *Cardiovasc Res* **59:**824–833.

Bulau P, Zakrzewicz D, Kitowska K, Leiper J, Gunther A, Grimminger F, and Eickelberg O (2007) Analysis of methylarginine metabolism in the cardiovascular system identifies the lung as a major source of ADMA. *Am J Physiol Lung Cell Mol Physiol* **292:**L18–L24.

Cariou B and Staels B (2007) FXR: a promising target for the metabolic syndrome? *Trends Pharmacol Sci* **28:**236–243.

Cariou B, van Harmelen K, Duran-Sandoval D, van Dijk TH, Grefhorst A, Abdelkarim M, Caron S, Torpier G, Fruchart JC, Gonzalez FJ, et al. (2006) The farnesoid X receptor modulates adiposity and peripheral insulin sensitivity in mice. *J Biol Chem* **281:**11039–11049.

Dudzinski DM, Igarashi J, Greif D, and Michel T (2006) The regulation and pharmacology of endothelial nitric oxide synthase. *Annu Rev Pharmacol Toxicol* **46:**235–276.

Echchgadda I, Song CS, Roy AK, and Chatterjee B (2004) Dehydroepiandrosterone sulfotransferase is a target for transcriptional induction by the vitamin D receptor. *Mol Pharmacol* **65:**720–729.

Eloranta JJ and Kullak-Ublick GA (2005) Coordinate transcriptional regulation of bile acid homeostasis and drug metabolism. *Arch Biochem Biophys* **433:**397–412.

Gary JD and Clarke S (1998) RNA and protein interactions modulated by protein arginine methylation. *Prog Nucleic Acid Res Mol Biol* **61:**65–131.

Hasegawa K, Wakino S, Tatematsu S, Yoshioka K, Homma K, Sugano N, Kimoto M, Hayashi K, and Itoh H (2007) Role of asymmetric dimethylarginine in vascular injury in transgenic mice overexpressing dimethylarginine dimethylaminohydrolase 2. *Circ Res* **101:**e2–e10.

Hatzoglou M, Fernandez J, Yaman I, and Closs E (2004) Regulation of cationic amino acid transport: the story of the CAT-1 transporter. *Annu Rev Nutr* **24:**377–399.

He F, Li J, Mu Y, Kuruba R, Ma Z, Wilson A, Alber S, Jiang Y, Stevens T, Watkins S, et al. (2006) Downregulation of endothelin-1 by farnesoid X receptor in vascular endothelial cells. *Circ Res* **98:**192–199.

Hu T, Chouinard M, Cox AL, Sipes P, Marcelo M, Ficorilli J, Li S, Gao H, Ryan TP, Michael MD, et al. (2006) Farnesoid X receptor agonist reduces serum asymmetric dimethylarginine levels through hepatic dimethylarginine dimethylaminohydrolase-1 gene regulation. *J Biol Chem* **281:**39831–39838.

Jung D, Mangelsdorf DJ, and Meyer UA (2006) Pregnane X receptor is a target of farnesoid X receptor. *J Biol Chem* **281:**19081–19091.

Kielstein JT and Zoccali C (2008) Asymmetric dimethylarginine: a novel marker of risk and a potential target for therapy in chronic kidney disease. *Curr Opin Nephrol Hypertens* **17:**609–615.

Kocarek TA, Shenoy SD, Mercer-Haines NA, and Runge-Morris M (2002) Use of dominant negative nuclear receptors to study xenobiotic-inducible gene expression in primary cultured hepatocytes. *J Pharmacol Toxicol Methods* **47:**177–187.

Leiper J, Nandi M, Torondel B, Murray-Rust J, Malaki M, O'Hara B, Rossiter S,

Anthony S, Madhani M, Selwood D, et al.(2007) Disruption of methylarginine metabolism impairs vascular homeostasis. *Nat Med* **13:**198–203.
Li J, Wilson A, Kuruba R, Zhang Q, Gao X, He F, Zhang LM, Pitt BR, Xie W, and Li S (2008) FXR-mediated regulation of eNOS expression in vascular endothelial cells. *Cardiovasc Res* **77:**169–177.
Maloney PR, Parks DJ, Haffner CD, Fivush AM, Chandra G, Plunket KD, Creech KL, Moore LB, Wilson JG, Lewis MC, et al. (2000) Identification of a chemical tool for the orphan nuclear receptor FXR. *J Med Chem* **43:**2971–2974.
Mann GE, Yudilevich DL, and Sobrevia L (2003) Regulation of amino acid and glucose transporters in endothelial and smooth muscle cells. *Physiol Rev* **83:**183–252.
Martens-Lobenhoffer J, Krug O, and Bode-Böger SM (2004) Determination of arginine and asymmetric dimethylarginine (ADMA) in human plasma by liquid chromatography/mass spectrometry with the isotope dilution technique. *J Mass Spectrom* **39:**1287–1294.
Monsalve E, Oviedo PJ, García-Pérez MA, Tarín JJ, Cano A, and Hermenegildo C (2007) Estradiol counteracts oxidized LDL-induced asymmetric dimethylarginine production by cultured human endothelial cells. *Cardiovasc Res* **73:**66–72.
Palm F, Onozato ML, Luo Z, and Wilcox CS (2007) Dimethylarginine dimethylaminohydrolase (DDAH): expression, regulation, and function in the cardiovascular and renal systems. *Am J Physiol Heart Circ Physiol* **293:**H3227–H3245.
Podvinec M, Kaufmann MR, Handschin C, and Meyer UA (2002) NUBIScan, an in silico approach for prediction of nuclear receptor response elements. *Mol Endocrinol* **16:**1269–1279.
Reade MC, Clark MF, Young JD, and Boyd CA (2002) Increased cationic amino acid flux through a newly expressed transporter in cells overproducing nitric oxide from patients with septic shock. *Clin Sci* **102:**645–650.
Schulz E, Jansen T, Wenzel P, Daiber A, and Münzel T (2008) Nitric oxide, tetrahydrobiopterin, oxidative stress, and endothelial dysfunction in hypertension. *Antioxid Redox Signal* **10:**1115–1126.
Searles CD (2006) Transcriptional and posttranscriptional regulation of endothelial nitric oxide synthase expression. *Am J Physiol Cell Physiol* **291:**C803–C816.
Shaul PW (2002) Regulation of endothelial nitric oxide synthase: location, location, location. *Annu Rev Physiol* **64:**749–774.
Siroen MP, van Leeuwen PA, Nijveldt RJ, Teerlink T, Wouters PJ, and Van den Berghe G (2005) Modulation of asymmetric dimethylarginine in critically ill patients receiving intensive insulin treatment: a possible explanation of reduced morbidity and mortality? *Crit Care Med* **33:**504–510.
Stamler JS and Feelisch M (1996) Preparation and detection of *S*-nitrosothiols, in *Methods in Nitric Oxide Research* (Feelisch M and Stamler JS eds) pp 521–539, John Wiley & Sons, New York.
Stuehr DJ (1997) Structure-function aspects in the nitric oxide synthases. *Annu Rev Pharmacol Toxicol* **37:**339–359.
Tain YL and Baylis C (2007) Determination of dimethylarginine dimethylaminohydrolase activity in the kidney. *Kidney Int* **72:**886–889.
Teerlink T (2005) ADMA metabolism and clearance. *Vasc Med* **10:**S73–S81.
Vallance P and Leiper J (2004) Cardiovascular biology of the asymmetric dimethylarginine:dimethylarginine dimethylaminohydrolase pathway. *Arterioscler Thromb Vasc Biol* **24:**1023–1030.
Watanabe M, Houten SM, Wang L, Moschetta A, Mangelsdorf DJ, Heyman RA, Moore DD, and Auwerx J (2004) Bile acids lower triglyceride levels via a pathway involving FXR, SHP, and SREBP-1c. *J Clin Invest* **113:**1408–1418.
Wilson Tang WH, Tong W, Shrestha K, Wang Z, Levison BS, Delfraino B, Hu B, Troughton RW, Klein AL, and Hazen SL (2008) Differential effects of arginine methylation on diastolic dysfunction and disease progression in patients with chronic systolic heart failure. *Eur Heart J* **29:**2506–2513.

Address correspondence to: Dr. Song Li, Center for Pharmacogenetics, Department of Pharmaceutical Sciences, University of Pittsburgh School of Pharmacy, 639 Salk Hall, Pittsburgh, PA 15261. E-mail: sol4@pitt.edu